

A NEW RECONSTRUCTION METHOD FOR THE INVERSE POTENTIAL PROBLEM

A. CANELAS, A. LAURAIN, AND A. A. NOVOTNY

ABSTRACT. The inverse potential problem consists in reconstructing an unknown measure with support in a geometrical domain from a single boundary measurement. In order to deal with this severely ill-posed inverse problem, we rewrite it as an optimization problem where a Kohn-Vogelius-type functional measuring the misfit between the solutions of two auxiliary problems is minimized. One auxiliary problem contains information on the boundary measurement while the other one corresponds to the boundary excitation. The solutions of the auxiliary problems coincide once the inverse problem is solved. In order to minimize the Kohn-Vogelius criterion, its total variation with respect to a set of ball-shaped perturbations on the measure is explicitly evaluated. Then, a new method for solving the inverse potential problem based on the expression obtained is devised. Finally, some numerical results are presented in order to show the effectiveness of the devised reconstruction algorithm.

1. INTRODUCTION

The inverse potential problem consists in reconstructing an unknown measure with support in a domain Ω from a single measurement of its potential on the boundary $\partial\Omega$. This problem has important applications such as gravimetry, where the goal is to determine Earth's density distribution from the measurement of the gravity and its derivatives on the surface of the Earth.

The inverse potential problem is notoriously ill-posed. The notion of well-posedness due to Hadamard requires the existence and uniqueness of a solution and the continuity of the inverse mapping. In the inverse potential problem, uniqueness and continuity of the inverse mapping are not at hand, the latter being responsible for the instability of the reconstruction process. Additional practical issues such as partial measurement render the inverse problem even more difficult.

To deal with the problem of uniqueness, a priori assumptions on the class of measures to be reconstructed can be made. This question has been thoroughly studied from a theoretical point of view by Isakov [15]. He exhibits several classes of densities such that the reconstruction process admits a unique solution. For instance, one can show the uniqueness of the reconstruction when the intensity is fixed and the support of the density is star-shaped with respect to its barycenter.

Even with such assumptions the stability of the reconstruction is an issue, in particular in the presence of noise which is commonplace in practice. A standard approach to deal with inverse problems consists in introducing a regularization of the inverse operator. Many choices for the regularization are available which may dramatically affect the reconstruction. A typical example is the Tikhonov regularization based on the L^2 -norm of the unknown, which has a strong smoothing effect. These methods are easy to handle but tend to provide a smooth solution, which is not suited to reconstruct piecewise smooth structures. However, such piecewise smooth structures are very often encountered in practice as in geology and imaging for instance, and a different approach is then necessary. A possible approach is to use a total variation (TV) regularization, which corresponds to the L^1 -norm of the gradient for continuously differentiable functions. This approach has been successfully employed for many inverse problems to reconstruct piecewise smooth structures, including the problem of gravimetry [7].

A more direct approach consists in looking for the geometry of the support of the density, assuming the intensity is known, which is a reasonable assumption for many applications. This yields a shape/topology optimization problem in the sense that we are looking for an unknown

Key words and phrases. inverse potential problem, Kohn-Vogelius criterion, total variation, reconstruction method.

set/interface/topology inside Ω : the support of the density. This approach has been successfully used for inverse problems; see [1, 4, 8, 9, 11, 2, 10, 12, 13, 14, 19]. In the context of gravimetry, this approach has been employed using a level-set method to represent the domains [17, 21]. The successful application of the so-called topological derivative [20] for solving a class of inverse problems should also be noted. The topological derivative can be used either as a standalone tool to accurately and quickly detect a density with a small support, even with several connected components, or as an initialization for a level-set method such as in [17, 21].

In our paper the inverse problem is reformulated as an optimization problem, where the support of the measure is the unknown variable. The topology optimization problem consists in minimizing the so-called Kohn-Vogelius functional [18], which measures the misfit between the solutions of two auxiliary problems. One auxiliary problem contains information on the boundary measurement while the other one corresponds to the boundary excitation. The solutions of the auxiliary problems coincide once the inverse problem is solved. The total variation of the Kohn-Vogelius criterion, with respect to a set of ball-shaped perturbations on the measure, is then explicitly evaluated. From the expansion obtained, a new method for solving the inverse potential problem is proposed. We note that in the present topology optimization approach there is no regularization term in the functional to be minimized. Regularization instead comes from the class of trial functions used for the minimization process.

The paper is organized as follows. In Section 2 we formulate the inverse source problem. In Section 3 the total variation of the Kohn-Vogelius criterion is explicitly derived. Finally, in Section 4 we devise a reconstruction algorithm and present several numerical examples.

2. PROBLEM FORMULATION

Let $\Omega \subset \mathbb{R}^2$ be an open and bounded domain, with Lipschitz boundary $\partial\Omega$. Consider the following over-determined boundary value problem:

$$\left\{ \begin{array}{l} -\Delta u = b^* \quad \text{in } \Omega, \\ u = u^* \\ -\partial_n u = q^* \end{array} \right\} \quad \text{on } \partial\Omega. \quad (2.1)$$

The inverse potential problem reads: given $q^* \in H^{-1/2}(\partial\Omega)$ and $u^* \in H^{1/2}(\partial\Omega)$, find the unknown source $b^* \in PC_\gamma(\Omega)$ such that there exists $u \in H^1(\Omega)$ satisfying (2.1), with

$$PC_\gamma(\Omega) := \{b \in L^\infty(\Omega), b = \gamma_0 \chi_{\Omega \setminus \omega} + \gamma_1 \chi_\omega \mid \omega \subset \Omega \text{ is measurable}\}. \quad (2.2)$$

In (2.2) χ_ω denotes the indicator function of the set ω and $\gamma = (\gamma_0, \gamma_1) \in \mathbb{R}^2$ is given.

It is known that this inverse source problem is severely ill-posed and additional boundary measurements (of higher-order derivatives of the potential) do not provide further information for the reconstruction; see [16]. The ill-posedness is due, on one hand, to the lack of uniqueness of the solution and on the other hand to the lack of stability of the reconstruction. The lack of uniqueness for this problem is severe, and one needs to choose a small set of admissible functions to restore it. These questions were studied thoroughly in [15], where several classes of functions are shown to provide uniqueness. For instance, it is not possible to determine both the support ω^* and the intensities $\gamma = (\gamma_0, \gamma_1)$ of the source b^* . Therefore, we assume that the intensities (γ_0, γ_1) are given and attempt to reconstruct the support ω^* from the boundary measurement. Even with known intensities γ , there is non-uniqueness of the solution ω^* , i.e. different supports ω^* may produce the same boundary data (u^*, q^*) . Examples of this nature are easy to provide, for instance a ring ω^* produces the same boundary data as a disk with identical barycenter and area. Therefore, additional geometrical constraints are necessary to obtain uniqueness. A useful example of such a class is given in [15, 17]:

Theorem 1. *Assume $b_i = \gamma_0 \chi_{\Omega \setminus \omega_i} + \gamma_1 \chi_{\omega_i} \in PC_\gamma(\Omega)$, $i = 1, 2$ where $\gamma = (\gamma_0, \gamma_1)$ is given, and ω_1, ω_2 are two star-shaped domains with respect to their barycenters. If the corresponding boundary data in (2.1) are equal, then $\omega_1 = \omega_2$.*

The condition of star-shapedness in Theorem 1 is rather restrictive, in particular since it requires the set ω to be connected. It is actually only a sufficient condition, since uniqueness

could be achieved for a broader class of sets. It is however difficult to describe the maximal class of domains for which uniqueness holds. Therefore, in this paper we consider a broader class of admissible sets for which we usually obtain excellent numerical reconstructions: let $m > 0$ be a given integer, and $\mathcal{I} = \{1, \dots, m\}$. We assume that the sets ω in $PC_\gamma(\Omega)$ are of the form:

$$\omega = \bigcup_{i \in \mathcal{I}} \omega_i \quad \text{with} \quad \omega_i \cap \omega_j = \emptyset \quad \text{for} \quad i \neq j. \quad (2.3)$$

where each ω_i is measurable and simply connected; see Figure 1.

The other issue of the inverse source problem is stability. As explained in the introduction, this issue requires regularization of the inverse operator. In an optimization approach, this can be achieved by adding a regularizing term to the objective function, such as in the Tikhonov or the TV approaches. In our approach, the regularization is obtained by restricting the class of admissible sets ω to a finite set of balls with varying sizes; see Section 4.

To address the inverse problem (2.1), we reformulate it as an optimization problem. This is done by minimizing the misfit between the solutions of the Dirichlet and the Neumann problems, i.e. we minimize the so-called Kohn-Vogelius functional [18]:

$$\min_{b \in PC_\gamma(\Omega)} J(b) := \frac{1}{2} \int_{\Omega} (u^D[b] - u^N[b])^2, \quad (2.4)$$

where $u^D[b]$ and $u^N[b]$ are solutions to the following auxiliary problems:

$$\begin{cases} -\Delta u^D[b] = b & \text{in } \Omega, \\ u^D[b] = u^* & \text{on } \partial\Omega, \end{cases} \quad \text{and} \quad (2.5)$$

$$\begin{cases} -\Delta u^N[b] = b + c[b] & \text{in } \Omega, \\ -\partial_n u^N[b] = q^* & \text{on } \partial\Omega, \\ \int_{\Omega} u^N[b] = \int_{\Omega} u^D[b], \end{cases} \quad (2.6)$$

where the constant $c[b]$ is introduced in order to satisfy the compatibility condition of the Neumann problem:

$$c[b] = \frac{1}{|\Omega|} \left(\int_{\partial\Omega} q^* - \int_{\Omega} b \right). \quad (2.7)$$

On one hand, if $b = b^*$ then we obviously have $J(b) = 0$. On the other hand if $b \in PC_\gamma(\Omega)$ satisfies $J(b) = 0$, then $u^D[b] = u^N[b]$, which implies $c[b] = 0$ and then $u^D[b] = u^N[b]$ solves the over-determined problem (2.1). However this does not imply $b = b^*$ due to the lack of uniqueness of the inverse source problem discussed above. At least one can show that ω in $b = \gamma_0 \chi_{\Omega \setminus \omega} + \gamma_1 \chi_{\omega}$ has the same moments as the target domain ω^* , in particular it has the same barycenter $x = x^*$ and volume $|\omega| = |\omega^*|$, where

$$|\omega^*| := \frac{1}{\gamma_1 - \gamma_0} \left[\int_{\partial\Omega} q^* - \gamma_0 |\Omega| \right], \quad (2.8)$$

$$x^* := \frac{1}{(\gamma_1 - \gamma_0) |\omega^*|} \left[\int_{\partial\Omega} (q^* x + u^* n) - \gamma_0 \int_{\Omega} x \right]. \quad (2.9)$$

Nevertheless, in practice we are usually able to reconstruct the true measure even if it has several connected components, which seems to indicate that uniqueness of the reconstruction could be obtained for a broader class of measures than the star-shaped domains of Theorem 1.

3. RECONSTRUCTION METHOD

To devise an effective reconstruction method, we first evaluate explicitly the total variation of the Kohn-Vogelius criterion with respect to a set of ball-shaped perturbations on the measure. In order to introduce these ideas, let us consider a non-smooth perturbation of $\mathcal{J}(\Omega)$ confined in a small set $\varpi_{\varepsilon, \hat{x}} = \hat{x} + \varepsilon \varpi$ of size $\varepsilon > 0$, or the union $\varpi_{\mathbf{e}, \hat{\mathbf{x}}} := \cup_{i \in \mathcal{I}} \varpi_{\varepsilon_i, \hat{x}_i}$ of such sets, where

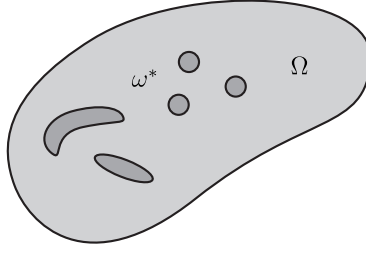


FIGURE 1. The inverse potential problem.

$\mathbf{e} := \{\varepsilon_i\}_{i \in \mathcal{I}}$, $\hat{\mathbf{x}} := \{\hat{x}_i\}_{i \in \mathcal{I}}$. Here, $\hat{x}_i \in \Omega$ and $\varpi \subset \mathbb{R}^2$, with $0 \in \varpi$, is fixed. We introduce an expansion of the Kohn-Vogelius shape functional $\mathcal{J}(\Omega \setminus \varpi_{\mathbf{e}, \hat{\mathbf{x}}})$ of the form

$$\mathcal{J}(\Omega \setminus \varpi_{\mathbf{e}, \hat{\mathbf{x}}}) = \mathcal{J}(\Omega) + \sum_{i \in \mathcal{I}} f_1(\varepsilon_i) D^1 \mathcal{J}(\hat{x}_i) + \sum_{i, j \in \mathcal{I}} f_2(\varepsilon_i, \varepsilon_j) D^2 \mathcal{J}(\hat{x}_i, \hat{x}_j) + \mathcal{R}(\mathbf{e}, \hat{\mathbf{x}}), \quad (3.1)$$

where $f_1(\varepsilon_i)$ and $f_2(\varepsilon_i, \varepsilon_j)$ are positive functions such that

$$\lim_{\varepsilon_i \rightarrow 0} f_1(\varepsilon_i) = 0, \quad \lim_{\varepsilon_i, \varepsilon_j \rightarrow 0} \frac{f_2(\varepsilon_i, \varepsilon_j)}{f_1(\varepsilon_i)} = 0 \quad \text{and} \quad \lim_{\mathbf{e} \rightarrow 0} \frac{\mathcal{R}(\mathbf{e}, \hat{\mathbf{x}})}{f_2(\varepsilon_i, \varepsilon_j)} = 0 \quad \forall i, j \in \mathcal{I}. \quad (3.2)$$

We call first and second order derivatives of \mathcal{J} to the functions $D^1 \mathcal{J}$ and $D^2 \mathcal{J}$, respectively, of the expansion (3.1).

3.1. Perturbed problems. For our purposes, let us consider the particular case $\varpi_{\mathbf{e}, \hat{\mathbf{x}}} = \cup_{i \in \mathcal{I}} B(\varepsilon_i, \hat{x}_i)$, where $B(\varepsilon_i, \hat{x}_i)$ is a disk of radius ε_i and center $\hat{x}_i \in \Omega$. We consider a source term of the form

$$b_{\mathbf{e}, \hat{\mathbf{x}}} = \gamma_0 \chi_{\Omega \setminus \varpi_{\mathbf{e}, \hat{\mathbf{x}}}} + \gamma_1 \sum_{i \in \mathcal{I}} \chi_{B(\varepsilon_i, \hat{x}_i)}. \quad (3.3)$$

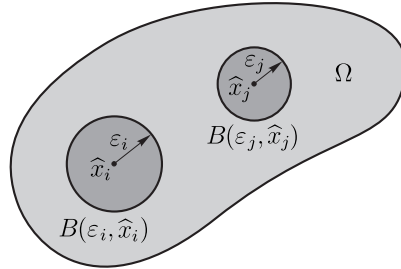


FIGURE 2. Ball-shaped perturbations.

The perturbed shape functional is written as

$$\mathcal{J}(\Omega \setminus \varpi_{\mathbf{e}, \hat{\mathbf{x}}}) := J(b_{\mathbf{e}, \hat{\mathbf{x}}}) = \frac{1}{2} \int_{\Omega} (u^D[b_{\mathbf{e}, \hat{\mathbf{x}}}] - u^N[b_{\mathbf{e}, \hat{\mathbf{x}}}]^2), \quad (3.4)$$

where $u^D[b_{\mathbf{e}, \hat{\mathbf{x}}}]$ and $u^N[b_{\mathbf{e}, \hat{\mathbf{x}}}]$ are solutions of

$$\begin{cases} -\Delta u^D[b_{\mathbf{e}, \hat{\mathbf{x}}}] = b_{\mathbf{e}, \hat{\mathbf{x}}} & \text{in } \Omega, \\ u^D[b_{\mathbf{e}, \hat{\mathbf{x}}}] = u^* & \text{on } \partial\Omega, \end{cases} \quad (3.5)$$

$$\begin{cases} -\Delta u^N[b_{\mathbf{e}, \hat{\mathbf{x}}}] = b_{\mathbf{e}, \hat{\mathbf{x}}} + c[b_{\mathbf{e}, \hat{\mathbf{x}}}] & \text{in } \Omega, \\ -\partial_n u^N[b_{\mathbf{e}, \hat{\mathbf{x}}}] = q^* & \text{on } \partial\Omega, \\ \int_{\Omega} u^N[b_{\mathbf{e}, \hat{\mathbf{x}}}] = \int_{\Omega} u^D[b_{\mathbf{e}, \hat{\mathbf{x}}}], \end{cases} \quad (3.6)$$

with the constant $c[b_{\mathbf{e}, \widehat{\mathbf{x}}}]$ obtained from the compatibility condition:

$$c[b_{\mathbf{e}, \widehat{\mathbf{x}}}] = \frac{1}{|\Omega|} \left(\int_{\partial\Omega} q^* - \int_{\Omega} b_{\mathbf{e}, \widehat{\mathbf{x}}} \right) = c[\gamma_0] - \frac{\gamma_1 - \gamma_0}{|\Omega|} \sum_{i \in \mathcal{I}} \pi \varepsilon_i^2, \quad (3.7)$$

where $c[\gamma_0]$ is also computed using (2.7) with $b = \gamma_0$.

3.2. Explicit expansion of the Kohn-Vogelius criterion. In this section we present the derivation of the expansions for the functions $u^D[b_{\mathbf{e}, \widehat{\mathbf{x}}}]$ and $u^N[b_{\mathbf{e}, \widehat{\mathbf{x}}}]$. First, note that $u^D[b_{\mathbf{e}, \widehat{\mathbf{x}}}]$ can be expressed as

$$u^D[b_{\mathbf{e}, \widehat{\mathbf{x}}}] (x) = u^D[\gamma_0] (x) + \sum_{i \in \mathcal{I}} \pi \varepsilon_i^2 v_{\varepsilon_i} (x), \quad (3.8)$$

where each function v_{ε_i} is solution to

$$\begin{cases} -\Delta v_{\varepsilon_i} = \frac{\gamma_1 - \gamma_0}{\pi \varepsilon_i^2} \chi_{B(\varepsilon_i, \widehat{\mathbf{x}}_i)} & \text{in } \Omega, \\ v_{\varepsilon_i} = 0 & \text{on } \partial\Omega. \end{cases} \quad (3.9)$$

One may express v_{ε_i} as a sum of the form $v_{\varepsilon_i} = v_{\varepsilon_i}^p + v_{\varepsilon_i}^q$, where $v_{\varepsilon_i}^p$ is a particular solution obtained by using the fundamental solution of the Laplacian, namely:

$$v_{\varepsilon_i}^p (x) = \int_{B(\varepsilon_i, \widehat{\mathbf{x}}_i)} -\frac{\gamma_1 - \gamma_0}{\pi \varepsilon_i^2} \frac{1}{2\pi} \log \|y - x\| dy, \quad (3.10)$$

so that the remainder $v_{\varepsilon_i}^q := v_{\varepsilon_i} - v_{\varepsilon_i}^p$ is harmonic and compensates the discrepancy left by $v_{\varepsilon_i}^p$ on $\partial\Omega$, i.e. it solves the homogeneous boundary value problem:

$$\begin{cases} -\Delta v_{\varepsilon_i}^q = 0 & \text{in } \Omega, \\ v_{\varepsilon_i}^q = -v_{\varepsilon_i}^p & \text{on } \partial\Omega. \end{cases} \quad (3.11)$$

For $x \in \Omega \setminus \overline{B(\varepsilon_i, \widehat{\mathbf{x}}_i)}$ we can integrate (3.10) analytically to obtain

$$v_{\varepsilon_i}^p (x) = -\frac{\gamma_1 - \gamma_0}{2\pi} \log \|\widehat{\mathbf{x}}_i - x\| \quad \forall x \in \Omega \setminus \overline{B(\varepsilon_i, \widehat{\mathbf{x}}_i)}, \quad (3.12)$$

hence $v_{\varepsilon_i}^p (x)$ does not depend on ε_i for $x \in \Omega \setminus \overline{B(\varepsilon_i, \widehat{\mathbf{x}}_i)}$. Then, from (3.11) we observe that $v_{\varepsilon_i}^q$ does not depend on ε_i and since $v_{\varepsilon_i} = v_{\varepsilon_i}^p + v_{\varepsilon_i}^q$ we have that $v_{\varepsilon_i} (x)$ is also independent of ε_i for $x \in \Omega \setminus \overline{B(\varepsilon_i, \widehat{\mathbf{x}}_i)}$. For the Neumann problem we use the expansion:

$$u^N[b_{\mathbf{e}, \widehat{\mathbf{x}}}] (x) = u^N[\gamma_0] (x) + \sum_{i \in \mathcal{I}} \pi \varepsilon_i^2 [v_{\varepsilon_i} (x) + h_i (x)], \quad (3.13)$$

where the function h_i is solution to

$$\begin{cases} -\Delta h_i = -\frac{\gamma_1 - \gamma_0}{|\Omega|} & \text{in } \Omega, \\ -\partial_n h_i = g_i & \text{on } \partial\Omega, \\ \int_{\Omega} h_i = 0, \end{cases} \quad (3.14)$$

where $g_i = \partial_n v_{\varepsilon_i}$ on $\partial\Omega$ is actually independent of ε_i according to the previous comments, with v_{ε_i} solution to (3.9).

Therefore, the expansion of the Kohn-Vogelius shape functional reads

$$\begin{aligned}
J(b_{\mathbf{e}, \hat{\mathbf{x}}}) &= \frac{1}{2} \int_{\Omega} (u^D[b_{\mathbf{e}, \hat{\mathbf{x}}}] - u^N[b_{\mathbf{e}, \hat{\mathbf{x}}}])^2 \\
&= \frac{1}{2} \int_{\Omega} \left[u^D[\gamma_0] + \sum_{i \in \mathcal{I}} \pi \varepsilon_i^2 v_{\varepsilon_i} - \left(u^N[\gamma_0] + \sum_{i \in \mathcal{I}} \pi \varepsilon_i^2 (v_{\varepsilon_i} + h_i) \right) \right]^2 \\
&= \frac{1}{2} \int_{\Omega} \left[(u^D[\gamma_0] - u^N[\gamma_0]) - \sum_{i \in \mathcal{I}} \pi \varepsilon_i^2 h_i \right]^2 \\
&= \frac{1}{2} \int_{\Omega} (u^D[\gamma_0] - u^N[\gamma_0])^2 \\
&\quad - \int_{\Omega} (u^D[\gamma_0] - u^N[\gamma_0]) \sum_{i \in \mathcal{I}} \pi \varepsilon_i^2 h_i + \frac{1}{2} \int_{\Omega} \left(\sum_{i \in \mathcal{I}} \pi \varepsilon_i^2 h_i \right)^2. \tag{3.15}
\end{aligned}$$

Proposition 2. *The expansion of the Kohn-Vogelius shape functional has the form*

$$\mathcal{J}(\Omega \setminus \varpi_{\mathbf{e}, \hat{\mathbf{x}}}) = \mathcal{J}(\Omega) - \int_{\Omega} (u^D[\gamma_0] - u^N[\gamma_0]) \sum_{i \in \mathcal{I}} \pi \varepsilon_i^2 h_i + \frac{1}{2} \int_{\Omega} \left(\sum_{i \in \mathcal{I}} \pi \varepsilon_i^2 h_i \right)^2, \tag{3.16}$$

i.e., the following terms of the general form (3.1) are promptly identified:

$$f_1(\varepsilon_i) = \pi \varepsilon_i^2, \quad f_2(\varepsilon_i, \varepsilon_j) = \frac{1}{2} \pi^2 \varepsilon_i^2 \varepsilon_j^2, \quad \mathcal{R}(\mathbf{e}, \hat{\mathbf{x}}) \equiv 0, \tag{3.17}$$

and

$$D^1 \mathcal{J}(\hat{x}_i) = - \int_{\Omega} (u^D[\gamma_0] - u^N[\gamma_0]) h_i, \quad D^2 \mathcal{J}(\hat{x}_i, \hat{x}_j) = \int_{\Omega} h_i h_j. \tag{3.18}$$

Remark 3. *Note that h_i depends on \hat{x}_i through the boundary data g_i in problem (3.14), since it also depends on \hat{x}_i through the source term in (3.9). Consequently (3.9) and (3.14) must be solved for each \hat{x}_i in order to evaluate the derivatives at \hat{x}_i .*

Let us introduce the adjoint states p^D and p^N solutions of

$$\begin{cases} -\Delta p^D &= -(u^D[\gamma_0] - u^N[\gamma_0]) & \text{in } \Omega, \\ p^D &= 0 & \text{on } \partial\Omega, \end{cases} \tag{3.19}$$

and

$$\begin{cases} -\Delta p^N &= u^D[\gamma_0] - u^N[\gamma_0] & \text{in } \Omega, \\ -\partial_n p^N &= 0 & \text{on } \partial\Omega, \\ \int_{\Omega} p^N &= 0, \end{cases} \tag{3.20}$$

(note that compatibility holds in (3.20) in view of (3.6)). From Green's formula, the first order derivative can be rewritten in its standard pointwise form, namely

$$D^1 \mathcal{J}(\hat{x}_i) = -(\gamma_1 - \gamma_0) (p^D(\hat{x}_i) + p^N(\hat{x}_i)). \tag{3.21}$$

3.3. Solution algorithm. When using perturbations of the type $\varpi_{\mathbf{e}, \hat{\mathbf{x}}} = \cup_{i \in \mathcal{I}} B(\varepsilon_i, \hat{x}_i)$, the shape optimization problem (2.4) is reduced to the minimization of $J(b_{\mathbf{e}, \hat{\mathbf{x}}})$ with respect to \mathbf{e} and $\hat{\mathbf{x}}$. We can introduce the change of variables $a_i := \pi \varepsilon_i^2, i \in \mathcal{I}$, and for a fixed point $\hat{\mathbf{x}}$ find the best areas minimizing $J_{\hat{\mathbf{x}}}(\mathbf{a}) := J(b_{\mathbf{e}, \hat{\mathbf{x}}})$. The following proposition shows the convenience of this approach:

Proposition 4. *The function $J_{\hat{\mathbf{x}}}(\mathbf{a})$ is a convex quadratic function of the variable \mathbf{a} . In addition, if the functions $\{h_i\}_{i \in \mathcal{I}}$, solutions to (3.14) for the points $\{\hat{x}_i\}_{i \in \mathcal{I}}$ are linearly independent, then $J_{\hat{\mathbf{x}}}(\mathbf{a})$ is a strictly convex quadratic function.*

Proof. This results follow from Proposition 2 and Theorems 3.3.7 and 3.3.8 in [6]. In effect, we have

$$J_{\widehat{\mathbf{x}}}(\mathbf{a}) = J_{\widehat{\mathbf{x}}}(\mathbf{0}) + \sum_{i \in \mathcal{I}} a_i D^1 \mathcal{J}(\widehat{x}_i) + \sum_{i, j \in \mathcal{I}} \frac{1}{2} a_i a_j D^2 \mathcal{J}(\widehat{x}_i, \widehat{x}_j), \quad (3.22)$$

then, the Hessian matrix of $J_{\widehat{\mathbf{x}}}(\mathbf{a})$ has components $D^2 \mathcal{J}(\widehat{x}_i, \widehat{x}_j)$. This matrix is positive semi-definite since, from (3.18)

$$\sum_{i, j \in \mathcal{I}} D^2 \mathcal{J}(\widehat{x}_i, \widehat{x}_j) a_i a_j = \int_{\Omega} \left(\sum_{i \in \mathcal{I}} a_i h_i \right)^2 \geq 0, \quad (3.23)$$

and is positive definite if the functions $\{h_i\}_{i \in \mathcal{I}}$ are linearly independent, since in this case the sum is zero only if $\mathbf{a} = 0$. \square

To find the optimal \mathbf{a} we differentiate (3.22) to obtain the first order optimality conditions:

$$\sum_{j \in \mathcal{I}} D^2 \mathcal{J}(\widehat{x}_i, \widehat{x}_j) a_j = -D^1 \mathcal{J}(\widehat{x}_i) \quad \text{for } i \in \mathcal{I}, \quad (3.24)$$

where $D^1 \mathcal{J}(\widehat{x}_i)$ is given by (3.21), and $D^2 \mathcal{J}(\widehat{x}_i, \widehat{x}_j)$ by (3.18). Note that from Proposition 4, the matrix of the linear system (3.24) is always positive semidefinite, and is positive definite if the functions $\{h_i\}_{i \in \mathcal{I}}$ are linearly independent. In this last case, the solution to (3.24) always exists, and is the unique global minimum of $J_{\widehat{\mathbf{x}}}(\mathbf{a})$.

We say that the point $\widehat{\mathbf{x}} = \{\widehat{x}_i\}_{i \in \mathcal{I}}$ is feasible if (3.24) has a meaningful solution in the sense that $a_i > 0, i \in \mathcal{I}$. The numerical practice shows us that it is not necessary to consider additional constraints to avoid the overlapping between different balls or to have $\varpi_{\mathbf{e}, \widehat{\mathbf{x}}} \subset \Omega$. Meaningful solutions are found by imposing the positivity requirement only.

At a feasible point we define $\mathbf{e}(\widehat{\mathbf{x}}) := \{\sqrt{a_i/\pi}\}_{i \in \mathcal{I}}$ with $\{a_i\}_{i \in \mathcal{I}}$ solution to (3.24). The proposed approach is to optimize $J(b_{\mathbf{e}(\widehat{\mathbf{x}}), \widehat{\mathbf{x}}})$ with respect to $\widehat{\mathbf{x}}$ in a certain set of feasible points.

3.4. Example with a closed-form solution. Let us consider the disk $\Omega = \{x \in \mathbb{R}^2 \mid \|x\| < R\}$. We introduce the usual polar coordinate system that assigns the pair (r, θ) to the point $x = (x_1, x_2)$, so that $x_1 = r \cos(\theta)$, $x_2 = r \sin(\theta)$. Consider a generic point \widehat{x}_i of polar coordinates $(\widehat{r}_i, \widehat{\theta}_i)$ with $0 < \widehat{r}_i < R$ and let \widetilde{x}_i be the point of polar coordinates $(\widetilde{r}_i, \widetilde{\theta}_i)$ with $\widetilde{r}_i = R^2/\widehat{r}_i$ and $\widetilde{\theta}_i = \widehat{\theta}_i$. We define the functions $\widehat{s}_i(x) = \|x - \widehat{x}_i\|$, and $\widetilde{s}_i(x) = \|x - \widetilde{x}_i\|$. Then, for a circular perturbation of radius ε_i and center \widehat{x}_i , the solution to (3.9) is

$$v_{\varepsilon_i} = \begin{cases} \frac{(\gamma_1 - \gamma_0)}{2\pi} \left[\log \left(\frac{\widetilde{s}_i \widehat{r}_i}{\varepsilon_i R} \right) + \frac{\varepsilon_i^2 - \widetilde{s}_i^2}{2\varepsilon_i^2} \right] & \text{in } B(\varepsilon_i, \widehat{x}_i), \\ \frac{(\gamma_1 - \gamma_0)}{2\pi} \log \left(\frac{\widetilde{s}_i \widehat{r}_i}{\widetilde{s}_i R} \right) & \text{in } \Omega \setminus \overline{B(\varepsilon_i, \widehat{x}_i)}, \end{cases} \quad (3.25)$$

which can be proven by direct differentiation. The solution to (3.14) is

$$h_i = \frac{(\gamma_1 - \gamma_0)}{2\pi} \left[\frac{r^2}{2R^2} - \frac{1}{4} - 2 \log \left(\frac{\widetilde{s}_i}{\widetilde{r}_i} \right) \right]. \quad (3.26)$$

We can prove by direct differentiation the field equation and boundary condition of (3.14). In addition, since $\log(\widetilde{s}_i/\widetilde{r}_i)$ is harmonic, by the mean value property of harmonic functions, we have

$$\int_0^{2\pi} r \left[\log \left(\frac{\widetilde{s}_i}{\widetilde{r}_i} \right) \right] d\theta = 2\pi r \left[\log \left(\frac{\widetilde{s}_i}{\widetilde{r}_i} \right) \right]_{x=0} = 2\pi r \left[\log \left(\frac{\widetilde{r}_i}{\widetilde{r}_i} \right) \right] = 0. \quad (3.27)$$

Hence, by using this result we have

$$\begin{aligned} \int_{\Omega} h_i &= \frac{(\gamma_1 - \gamma_0)}{2\pi} \int_0^R \int_0^{2\pi} r \left[\frac{r^2}{2R^2} - \frac{1}{4} - 2 \log \left(\frac{\widetilde{s}_i}{\widetilde{r}_i} \right) \right] d\theta dr \\ &= \frac{(\gamma_1 - \gamma_0)}{2\pi} \cdot 2\pi \left[\frac{r^4}{8R^2} - \frac{r^2}{8} \right]_{r=0}^R = 0. \end{aligned} \quad (3.28)$$

The expressions for $\widehat{x}_i = 0$ can easily be obtained as:

$$v_{\varepsilon_i} = \begin{cases} \frac{(\gamma_1 - \gamma_0)}{2\pi} \left[\log \left(\frac{R}{\varepsilon_i} \right) + \frac{\varepsilon_i^2 - \widehat{s}_i^2}{2\varepsilon_i^2} \right] & \text{in } B(\varepsilon_i, 0), \\ \frac{(\gamma_1 - \gamma_0)}{2\pi} \log \left(\frac{R}{\widehat{s}_i} \right) & \text{in } \Omega \setminus \overline{B(\varepsilon_i, 0)}, \end{cases} \quad (3.29)$$

$$h_i = \frac{(\gamma_1 - \gamma_0)}{2\pi} \left[\frac{r^2}{2R^2} - \frac{1}{4} \right]. \quad (3.30)$$

We can see now that the functions $\{h_i\}_{i \in \mathcal{I}}$ are linearly independent. Let us assume, without loss of generality that $\widehat{x}_1 = 0$, i.e. the first point is at the origin. The case without points at the origin is simpler. Note that for any set of distinct points $\{\widehat{x}_i\}_{i \in \mathcal{I} \setminus \{1\}}$, we have a set of distinct points $\{\widetilde{x}_i\}_{i \in \mathcal{I} \setminus \{1\}}$. Consider the following linear combination:

$$\sum_{i \in \mathcal{I}} \alpha_i h_i = \left(\sum_{i \in \mathcal{I}} \alpha_i \right) \cdot \left(\frac{r^2}{2R^2} - \frac{1}{4} \right) - \sum_{i \in \mathcal{I} \setminus \{1\}} 2\alpha_i \log \left(\frac{\widetilde{s}_i}{\widetilde{r}_i} \right) = 0, \quad (3.31)$$

where we have omitted the irrelevant factor $(\gamma_1 - \gamma_0)/(2\pi)$. Since only the term $r^2/(2R^2) - 1/4$ has a nonzero Laplacian, the sum $\sum_{i \in \mathcal{I}} \alpha_i$ must be zero. Then we have

$$\sum_{i \in \mathcal{I} \setminus \{1\}} \alpha_i \log(\widetilde{s}_i) = \sum_{i \in \mathcal{I} \setminus \{1\}} \alpha_i \log(\widetilde{r}_i), \quad (3.32)$$

and the equality must hold at every point $x \in \Omega$. Since both the left and right hand sides in the above equation are harmonic, by the identity theorem of harmonic functions [22] both sides should be equally harmonically extended outside Ω . However, if any α_i , with $i > 1$, is not zero, then the left hand side is singular at \widetilde{x}_i , while the right hand side is not. Then, $\alpha_i = 0$, for each $i > 1$, and since $\sum_{i \in \mathcal{I}} \alpha_i = 0$ we also have $\alpha_1 = 0$. Then, the functions $\{h_i\}_{i \in \mathcal{I}}$ are linearly independent, and we can prove that the example has the following interesting property:

Proposition 5. *Consider the disk $\Omega = \{x \in \mathbb{R}^2 \mid \|x\| < R\}$. Then, the minimum of the Kohn-Vogelius functional (3.4) in the class*

$$A := \left\{ b_{\mathbf{e}, \widehat{\mathbf{x}}} = \gamma_0 \chi_{\Omega \setminus \varpi_{\mathbf{e}, \widehat{\mathbf{x}}}} + \gamma_1 \sum_{i=1}^n \chi_{B(\varepsilon_i, \widehat{x}_i)} \mid n \in \mathbb{N}, \widehat{x}_i \neq \widehat{x}_j \text{ for } i \neq j, \text{ and } \varpi_{\mathbf{e}, \widehat{\mathbf{x}}} \subset \Omega \right\}, \quad (3.33)$$

is unique. In particular, problem (2.4) can have at most one solution in A .

Proof. Assume that the Kohn-Vogelius functional has two minimal solutions in A , the first defined by the centers $\widehat{\mathbf{x}}_1 = \{\widehat{x}_1, \dots, \widehat{x}_n\}$ and radii $\mathbf{e}_1 = \{\varepsilon_1, \dots, \varepsilon_n\}$, and the second by the centers $\widehat{\mathbf{x}}_2 = \{\widehat{x}_{n+1}, \dots, \widehat{x}_{n+m}\}$ and radii $\mathbf{e}_2 = \{\varepsilon_{n+1}, \dots, \varepsilon_{n+m}\}$. Let the areas be $a_i = \pi \varepsilon_i^2$, $1 \leq i \leq n+m$, and without loss of generality assume that all the $n+m$ centers are distinct. Then, for the point $\widehat{\mathbf{x}} = \{\widehat{x}_1, \dots, \widehat{x}_{n+m}\}$, the vectors $(a_1, \dots, a_n, 0, \dots, 0)$ and $(0, \dots, 0, a_{n+1}, \dots, a_{n+m})$ should both be global minimal points of the function $J_{\widehat{\mathbf{x}}}(\mathbf{a})$ of (3.22) in the convex set defined by the linear constraints $a_i \geq 0$, $a_i \leq \pi(R - \|\widehat{x}_i\|)^2$, $1 \leq i \leq n+m$. However, since the functions $\{h_i\}_{i \in \mathcal{I}}$ are linearly independent, from Proposition 4 we obtain that $J_{\widehat{\mathbf{x}}}(\mathbf{a})$ is a strictly convex quadratic function of the variable \mathbf{a} , hence it has a unique global minimum in any convex set, see Theorem 3.4.2 in [6]. \square

Remark 6. *Note that the balls that define $b_{\mathbf{e}, \widehat{\mathbf{x}}} \in A$ can overlap. Hence A is not a subset of PC_γ . However, if uniqueness holds in A , then uniqueness holds on the smaller class $A \cap PC_\gamma$ (where the balls do not overlap) automatically.*

We end this section providing the analytic expressions of the second order derivative $D^2 \mathcal{J}(\widehat{x}_i, \widehat{x}_j)$. From (3.18) and (3.26) we have

$$D^2 \mathcal{J}(\widehat{x}_i, \widehat{x}_i) = \left[\frac{(\gamma_1 - \gamma_0)}{2\pi} \right]^2 \int_{\Omega} \left[\frac{r^2}{2R^2} - \frac{1}{4} - 2 \log \left(\frac{\widetilde{s}_i}{\widetilde{r}_i} \right) \right]^2, \quad (3.34)$$

and, by resorting again to the mean value property of harmonic functions we obtain

$$\begin{aligned} D^2 \mathcal{J}(\hat{x}_i, \hat{x}_i) &= \left[\frac{(\gamma_1 - \gamma_0)}{2\pi} \right]^2 \left\{ \int_{\Omega} \left[\frac{r^2}{2R^2} - \frac{1}{4} \right]^2 + \int_{\Omega} \left[2 \log \left(\frac{\tilde{s}_i}{\tilde{r}_i} \right) \right]^2 \right\} \\ &= \left[\frac{(\gamma_1 - \gamma_0)}{2\pi} \right]^2 \left\{ 2\pi \left[\frac{r^6}{24R^4} - \frac{r^4}{16R^2} + \frac{r^2}{32} \right]_{r=0}^R + 4 \int_{\Omega} \left[\log \left(\frac{\tilde{s}_i}{\tilde{r}_i} \right) \right]^2 \right\}. \end{aligned} \quad (3.35)$$

Hence, defining $f := \log(\tilde{s}_i/\tilde{r}_i)$ and the open set $\Omega_a := \{x \in \mathbb{R}^2 \mid \|x\| < a\}$, we are interested in computing the integral of f^2 on Ω_a for the particular value $a = R$. From Green's second identity we have

$$\int_{\Omega_a} f^2 \Delta g = \int_{\partial\Omega_a} f^2 \partial_n g - \int_{\partial\Omega_a} g \partial_n (f^2) + \int_{\Omega_a} g \Delta (f^2). \quad (3.36)$$

Since f is harmonic we have $\Delta(f^2) = 2\nabla f \cdot \nabla f = 2/\tilde{s}_i^2$, and by taking $g = 1/4(r^2 - a^2)$ we obtain

$$\int_{\Omega_a} f^2 = \int_{\partial\Omega_a} \frac{1}{2} a f^2 + \int_{\Omega_a} \frac{r^2 - a^2}{2\tilde{s}_i^2}, \quad (3.37)$$

where the last term is

$$\begin{aligned} \int_{\Omega_a} \frac{r^2 - a^2}{2\tilde{s}_i^2} &= \int_0^a r(r^2 - a^2) \int_0^{2\pi} \frac{1}{2\tilde{s}_i^2} d\theta dr \\ &= \int_0^a r(r^2 - a^2) \left[\frac{\arctan \left(\left(\frac{\tilde{r}_i + r}{\tilde{r}_i - r} \right) \cdot \tan \left(\frac{\theta}{2} \right) \right)}{\tilde{r}_i^2 - r^2} \right]_{\theta=0}^{2\pi} dr \\ &= \int_0^a r(r^2 - a^2) \cdot \frac{\pi}{\tilde{r}_i^2 - r^2} dr \\ &= -\frac{\pi}{2} [r^2 + \log(\tilde{r}_i^2 - r^2)(\tilde{r}_i^2 - a^2)]_{r=0}^a \\ &= -\frac{\pi}{2} \left[\log \left(\frac{\tilde{r}_i^2 - a^2}{\tilde{r}_i^2} \right) (\tilde{r}_i^2 - a^2) + a^2 \right]. \end{aligned} \quad (3.38)$$

Then, by defining ϕ as

$$\phi(r) = \int_0^{2\pi} \log \left(\frac{\tilde{s}_i}{\tilde{r}_i} \right)^2 d\theta, \quad (3.39)$$

(3.37) can be written as

$$\int_0^a r\phi(r) dr = \frac{1}{2} a^2 \phi(a) - \frac{\pi}{2} \left[\log \left(\frac{\tilde{r}_i^2 - a^2}{\tilde{r}_i^2} \right) (\tilde{r}_i^2 - a^2) + a^2 \right]. \quad (3.40)$$

By differentiating this last expression with respect to a we obtain

$$\frac{\partial \phi}{\partial a}(a) = -\frac{2\pi}{a} \log \left(\frac{\tilde{r}_i^2 - a^2}{\tilde{r}_i^2} \right). \quad (3.41)$$

From (3.39) we obtain $\phi(0) = 0$. Then, by integrating the previous expression we have

$$\begin{aligned} \phi(r) &= \int_0^r -\frac{2\pi}{a} \log \left(\frac{\tilde{r}_i^2 - a^2}{\tilde{r}_i^2} \right) da \\ &= \pi \left[\operatorname{dilog} \left(\frac{\tilde{r}_i^2 - a^2}{\tilde{r}_i^2} \right) \right]_{a=0}^r = \pi \operatorname{dilog} \left(\frac{\tilde{r}_i^2 - r^2}{\tilde{r}_i^2} \right). \end{aligned} \quad (3.42)$$

Then, from (3.37) and (3.40)

$$\int_{\Omega_a} f^2 = \frac{\pi a^2}{2} \left[\operatorname{dilog} \left(\frac{\tilde{r}_i^2 - a^2}{\tilde{r}_i^2} \right) - \log \left(\frac{\tilde{r}_i^2 - a^2}{\tilde{r}_i^2} \right) \cdot \left(\frac{\tilde{r}_i^2 - a^2}{a^2} \right) - 1 \right]. \quad (3.43)$$

Returning back to (3.35) and simplifying the expressions, we obtain

$$D^2 \mathcal{J}(\hat{x}_i, \hat{x}_i) = \frac{(\gamma_1 - \gamma_0)^2 R^2}{2\pi} \left[\operatorname{dilog} \left(\frac{\tilde{r}_i^2 - R^2}{\tilde{r}_i^2} \right) \right]$$

$$-\log\left(\frac{\tilde{r}_i^2 - R^2}{\tilde{r}_i^2}\right) \cdot \left(\frac{\tilde{r}_i^2 - R^2}{R^2}\right) - \frac{95}{96} \Big]. \quad (3.44)$$

Since $\tilde{r}_i = R^2/\hat{r}_i$, we can express the previous result as

$$D^2 \mathcal{J}(\hat{x}_i, \hat{x}_i) = \frac{(\gamma_1 - \gamma_0)^2 R^2}{4\pi} \cdot \left[2\varphi\left(\frac{\hat{r}_i^2}{R^2}\right) - \frac{95}{48} \right], \quad (3.45)$$

where

$$\varphi(x) = \operatorname{dilog}(1-x) - \frac{1-x}{x} \cdot \log(1-x), \quad (3.46)$$

is a positive continuous function in $(0, 1)$ satisfying

$$\lim_{x \rightarrow 0} \varphi(x) = 1, \quad \lim_{x \rightarrow 1} \varphi(x) = \frac{\pi^2}{6}. \quad (3.47)$$

If we consider another point \hat{x}_j of polar coordinates $(\hat{r}_j, \hat{\theta}_j)$ with $0 < \hat{r}_j < R$, by following similar steps as above we obtain

$$D^2 \mathcal{J}(\hat{x}_i, \hat{x}_j) = \frac{(\gamma_1 - \gamma_0)^2 R^2}{4\pi} \cdot \left[\varphi\left(\frac{\hat{r}_i \hat{r}_j}{R^2} e^{\iota \delta_{ij}}\right) + \varphi\left(\frac{\hat{r}_i \hat{r}_j}{R^2} e^{-\iota \delta_{ij}}\right) - \frac{95}{48} \right]. \quad (3.48)$$

where ι is the imaginary unit, and $\delta_{ij} = |\hat{\theta}_i - \hat{\theta}_j|$.

4. NUMERICAL RESULTS

We apply the algorithm described in Section 3.3 to several examples to demonstrate the effectiveness of the approach. We use the finite element method to solve the boundary value problems, and look for the optimal solution in the set of all the feasible points $\hat{\mathbf{x}} = \{\hat{x}_i\}_{i \in \mathcal{I}}$ where each \hat{x}_i belongs to a defined subgrid of the finite element grid (note that some combinations may be infeasible).

For the examples presented here, an exhaustive search in this set was used to find the optimal $\hat{\mathbf{x}}$. However, due to its computational complexity, the exhaustive search in the set of all combinations is possible only if the number of balls m is small, and other algorithms for combinatorial optimization problems should be used to address problems with a large m .

In the examples we take $\Omega = (0, 1) \times (0, 1)$, $\gamma_0 = 1$ and $\gamma_1 = 10$. The domain Ω is discretized with three-node finite elements. The mesh is generated from a grid of size 100×100 , where each resulting square is divided into four triangles, leading to 40×10^3 elements. Examples 1-5 are free of noise, while in Example 6 the data is corrupted with noise.

4.1. Example 1: Sensitivity with respect to the subgrid. Here we test the sensitivity of the reconstruction with respect to the size of the subgrid. We consider two subgrids of 10×10 and 20×20 nodes. From the result in Fig. 3, we note that the algorithm fails in finding accurately the location of the object in the coarse subgrid (Fig. 3b), while the reconstruction is much better for the fine subgrid (Fig. 3c). Therefore, the subgrid should be sufficiently fine in order to obtain a good reconstruction. Ideally, it should coincide with the finite element mesh. However, since the finite element mesh is usually very refined, such a fine subgrid is impracticable due to the combinatorial nature of the algorithm of Section 3.3. Therefore, we fix the subgrid to 20×20 nodes for the next examples, which leads to a good compromise between resolution and computational cost.

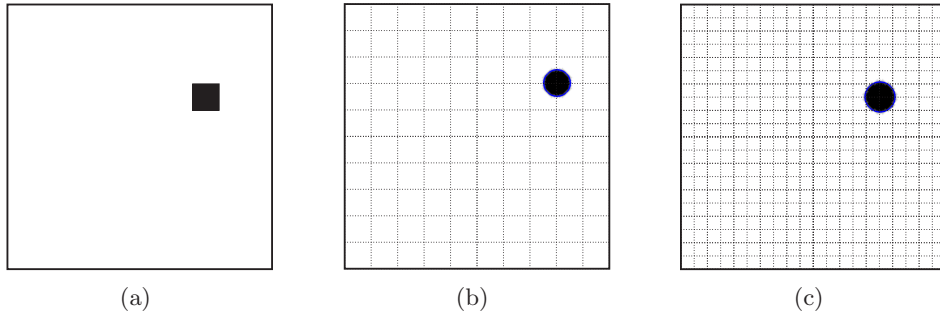


FIGURE 3. Sensitivity with respect to the subgrid: true source term (a) and reconstructions in a 10×10 (b) and 20×20 (c) subgrids.

4.2. Example 2: Sensitivity with respect to the contrast. We test the sensitivity with respect to the contrast $\gamma_1 - \gamma_0$. The true source term has intensity $\gamma_1 = 10$. Therefore, from the result in Fig. 4 we observe that for the intensity $\gamma_1 > 10$ the sizes of the anomalies are underestimated (Fig. 4b), while for the intensity $\gamma_1 < 10$ the sizes of the anomalies are overestimated (Fig. 4c). In both cases, the correct centers were found.

The result shows the adverse effect of the non-uniqueness mentioned in Sections 1 and 2. Anomalies produce similar boundary data when the product of their size and intensity is roughly the same.

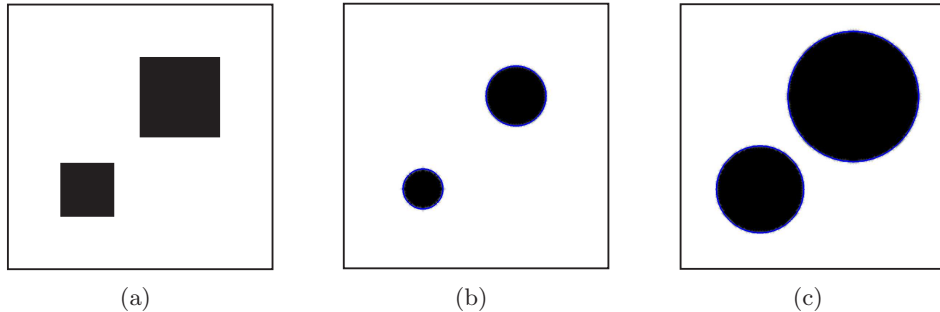


FIGURE 4. Sensitivity with respect to the contrast $\gamma_1 - \gamma_0$: true source term (a) and reconstructions for $\gamma_1 = 20$ (b) and $\gamma_1 = 5$ (c).

4.3. Example 3: Looking for the number of anomalies. We suppose that the number of anomalies is unknown and proceed with successive trials to find the correct number of balls m . We start with one trial ball and increment the number of balls every step until the algorithm provides the same result from one iteration to the next. In Figures 5, 6 and 7 we are looking for one, two and three anomalies, respectively. In the case of one anomaly, we start with one and end with two trial balls. With one trial ball we already reconstruct the anomaly, and with two trial balls we obtain the same result, i.e. the second trial (small) ball is embedded in the first one (Fig. 5) and we can conclude that there is only one main anomaly. For two anomalies, we start with two and end with three trial balls. We do not show the result for one trial ball since it is obviously inaccurate. Again, the results obtained for two and three balls are the same, i.e. the third trial (small) ball is included in one of the two others (Fig. 6), allowing us to conclude that there are two main anomalies. Finally, we proceed with three anomalies. The results for one and two trial balls are obvious. We conclude that there are three balls, since the results for three and four trial balls are identical (Fig. 7).

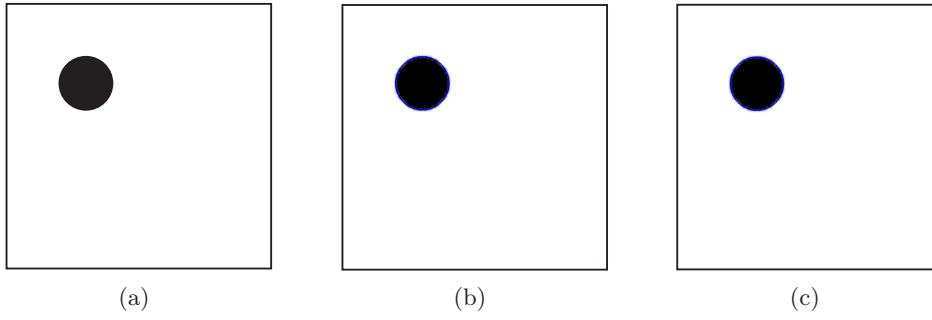


FIGURE 5. Looking for one anomaly: true source term (a) and reconstructions using one trial ball (b) and two trial balls (c).

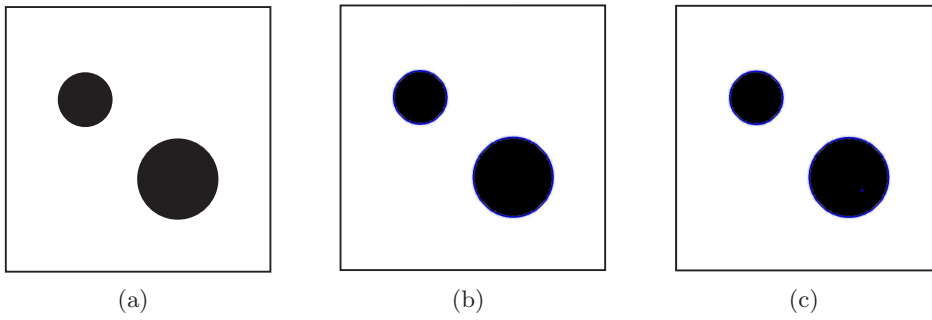


FIGURE 6. Looking for two anomalies: true source term (a) and reconstructions using two (b) and three trial balls (c).

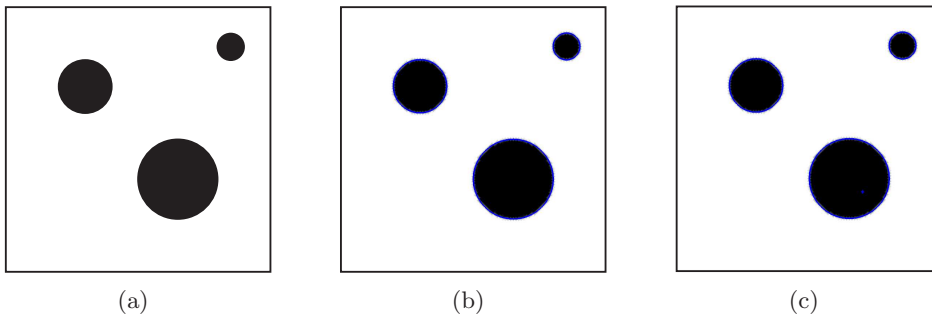


FIGURE 7. Looking for three anomalies: true source term (a) and reconstructions using three (b) and four trial balls (c).

4.4. Example 4: Shape and topology reconstruction. In this example we detect the topology as well as the shape of the anomalies. In the first case, the reconstruction of three square-shaped anomalies resulted in three balls, with approximately the same volume and barycenters, as shown in Fig. 8. The next result approximates two anomalies by three balls. Namely, in Fig. 9, the small square is approximated by one ball, while the rectangle is approximated by two balls. Finally, in Fig. 10, a L-shaped anomaly is approximated by three balls. Through these examples, we conclude that the proposed algorithm is able to reconstruct approximately the shape and the topology of hidden objects.

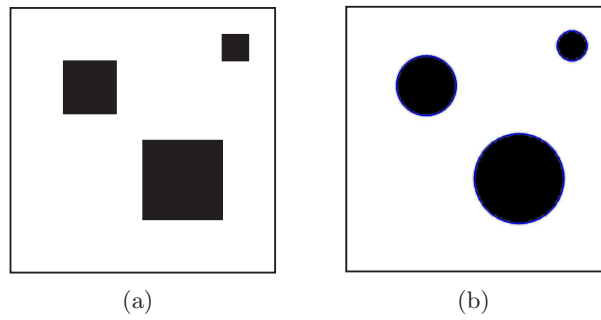


FIGURE 8. Three anomalies: true source term (a) and reconstruction using three balls (b).

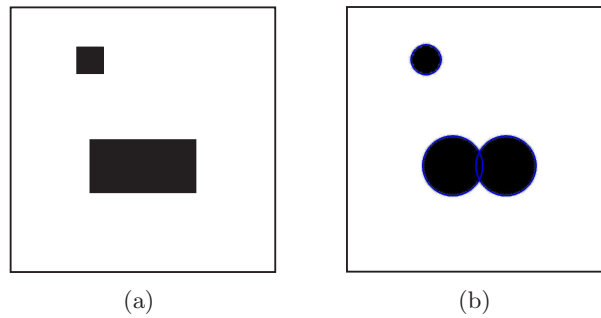


FIGURE 9. Two anomalies: true source term (a) and reconstruction using three balls (b).

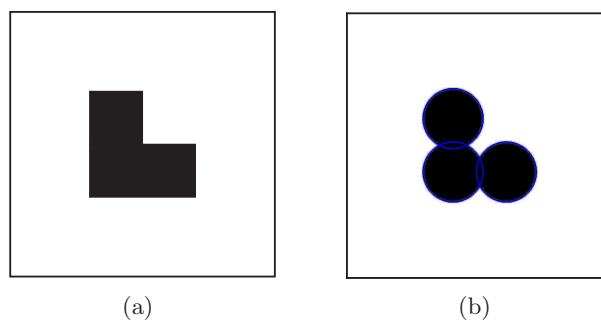


FIGURE 10. One anomaly: true source term (a) and reconstruction using three balls (b).

4.5. **Example 5: Anomalies of different sizes.** We consider two anomalies, where one of them is much bigger than the other one. In Fig. 11, we present the result for the anomalies far from each other. The case of anomalies very close to each other is shown in Figure 12. In both cases, the reconstructions match precisely the targets.

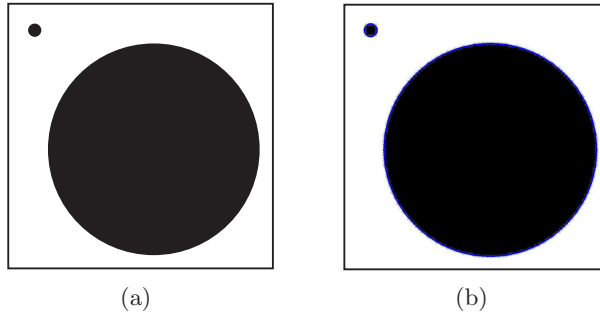


FIGURE 11. Two anomalies far from each other: true source term (a) and reconstruction using two balls (b).

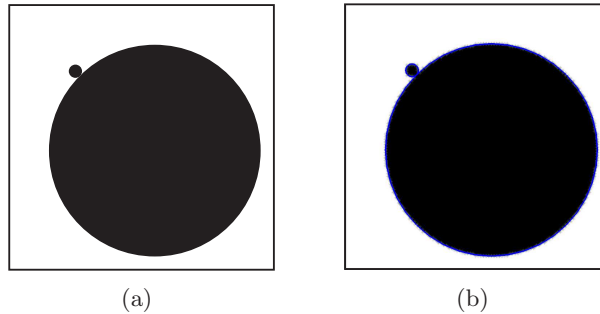


FIGURE 12. Two anomalies close to each other: true source term (a) and reconstruction using two balls (b).

4.6. Example 6: Detection of four simultaneous anomalies. Finally, we detect four simultaneous anomalies. In addition, we consider different levels of noise. In order to obtain noisy synthetic data, the true source term b^* is corrupted with white Gaussian noise, where the resulting level of noise on the boundary measurement is computed as follows

$$\text{noise} = \|q^* - q_n^*\|_{L^2(\partial\Omega)} / \|q^*\|_{L^2(\partial\Omega)} \times 100 \%, \quad (4.1)$$

where q_n^* is the noisy boundary measurement used as synthetic data. Through this procedure we can verify the robustness of the method with respect to noisy data avoiding, to some extent, the effect of the so called *inverse crime*. In Fig. 13, we present the target with four balls. The results obtained for different levels of noise are shown in Fig. 14. We observe that the results are acceptable until 4% of noise on the boundary measurement q^* . For 8% of noise, the true source term is completely degraded and the method fails in reconstructing b^* from the corrupted boundary measurement q_n^* .

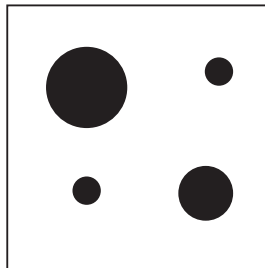


FIGURE 13. Four anomalies: true source term.

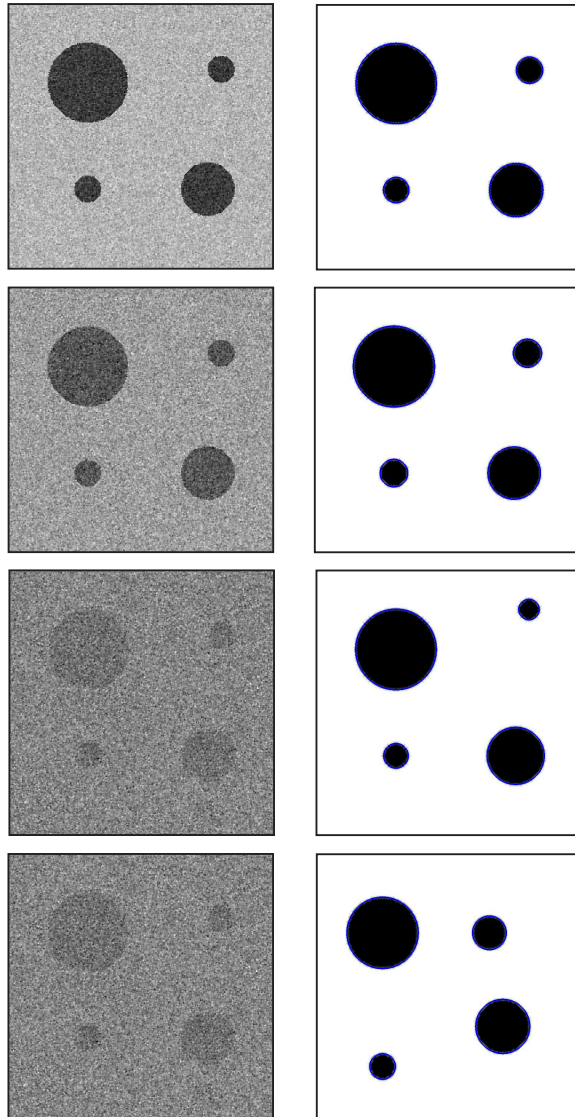


FIGURE 14. Four anomalies: noisy source term b^* (left) and reconstruction obtained using four balls (right), with 1.01%, 2.03%, 4.04% and 8.08% of resulting noise on q^* , respectively.

5. CONCLUSIONS

In this work, we have proposed a new method for solving the inverse potential problem. In particular, the inverse potential problem has been reformulated as an optimization problem using the Kohn-Vogelius criterion as objective function. In order to minimize the Kohn-Vogelius criterion, its total variation with respect to a set of ball-shaped perturbations on the unknown measure has been explicitly evaluated. We have proved that for this class of perturbations the expansion of the the Kohn-Vogelius criterion is exact up to the second order, i.e., there is no remainder. The expansion obtained has been used to minimize the Kohn-Vogelius criterion with respect to the size and center of the circular perturbations. This leads to an exhaustive combinatorial search which is tractable only in the case of a small number of unknown anomalies. Therefore, other algorithms for combinatorial optimization problems should be used to address problems with a large number of anomalies. Finally, we have presented an extensive set of numerical experiments showing the following features of the proposed reconstruction algorithm:

- The number of unknown anomalies can be found after some trials.
- The shape and topology of the unknown measure can be approximated by several balls.

- Anomalies of very different sizes (one anomaly much bigger than the other one, for instance) can be detected.
- Corrupted measurements with a high level of noise can be reconstructed with acceptable precision.

These promising results show that the application of other methods based on the expansion of a given shape functional, such as the simple iterative method proposed in [9] or the level-set method used in [5, 3], to the inverse potential problem should be investigated. In addition, since the proposed method can precisely approximate the unknown measure by several balls, it can be used to provide a good initial guess for other iterative methods such as the one studied in [17, 21].

ACKNOWLEDGEMENTS

We would like to thank Bojan Guzina for helpful comments on this paper. This research was partly supported by the Uruguayan Research Councils ANII and CSIC, and by the Brazilian Research Council CNPq. Antoine Laurain acknowledges financial support by the DFG Research Center Matheon “Mathematics for key technologies” through the MATHEON-Project C37 “Shape/Topology optimization methods for inverse problems”.

REFERENCES

- [1] H. Ammari, J. Garnier, V. Jugnon, and H. Kang. Stability and resolution analysis for a topological derivative based imaging functional. *SIAM J. Control Optim.*, 50(1):48–76, 2012.
- [2] Habib Ammari and Hyeonbae Kang. *Reconstruction of small inhomogeneities from boundary measurements*, volume 1846 of *Lecture Notes in Mathematics*. Springer-Verlag, Berlin, 2004.
- [3] S. Amstutz, S. M. Giusti, A. A. Novotny, and E. A. de Souza Neto. Topological derivative for multi-scale linear elasticity models applied to the synthesis of microstructures. *International Journal for Numerical Methods in Engineering*, 84:733–756, 2010.
- [4] S. Amstutz, I. Horchani, and M. Masmoudi. Crack detection by the topological gradient method. *Control and Cybernetics*, 34(1):81–101, 2005.
- [5] S. Amstutz, A. A. Novotny, and E. A. de Souza Neto. Topological derivative-based topology optimization of structures subject to Drucker-Prager stress constraints. *Computer Methods in Applied Mechanics and Engineering*, 233–236:123–136, 2012.
- [6] Mokhtar S. Bazaraa, Hanif D. Sherali, and C. M. Shetty. *Nonlinear programming*. Wiley-Interscience [John Wiley & Sons], Hoboken, NJ, third edition, 2006. Theory and algorithms.
- [7] H. Bertete-aguirre, E. Cherkaev, and M. Oristaglio. Non-smooth gravity problem with total variation penalization functional. *Geophysical Journal International*, 149:499–507, 2002.
- [8] M. Bonnet. Higher-order topological sensitivity for 2-D potential problems. *International Journal of Solids and Structures*, 46(11–12):2275–2292, 2009.
- [9] A. Canelas, A. A. Novotny, and J. R. Roche. A new method for inverse electromagnetic casting problems based on the topological derivative. *Journal of Computational Physics*, 230:3570–3588, 2011.
- [10] B. B. Guzina and I. Chikichev. From imaging to material identification: a generalized concept of topological sensitivity. *Journal of the Mechanics and Physics of Solids*, 55(2):245–279, 2007.
- [11] Bojan B. Guzina and Marc Bonnet. Small-inclusion asymptotic of misfit functionals for inverse problems in acoustics. *Inverse Problems*, 22(5):1761–1785, 2006.
- [12] M. Hintermüller and A. Laurain. Electrical impedance tomography: from topology to shape. *Control and Cybernetics*, 37(4):913–933, 2008.
- [13] M. Hintermüller and A. Laurain. Multiphase image segmentation and modulation recovery based on shape and topological sensitivity. *Journal of Mathematical Imaging and Vision*, 35:1–22, 2009.
- [14] M. Hintermüller, A. Laurain, and A. A. Novotny. Second-order topological expansion for electrical impedance tomography. *Advances in Computational Mathematics*, 36(2):235–265, 2012.
- [15] V. Isakov. *Inverse source problems*, volume 34 of *Mathematical Surveys and Monographs*. American Mathematical Society, Providence, RI, 1990.
- [16] V. Isakov. *Inverse problems for partial differential equations*. Springer, New York, 1998.
- [17] Victor Isakov, Shingyu Leung, and Jianliang Qian. A fast local level set method for inverse gravimetry. *Commun. Comput. Phys.*, 10(4):1044–1070, 2011.
- [18] R. Kohn and M. Vogelius. Determining conductivity by boundary measurements. *Comm. Pure Appl. Math.*, 37(3):289–298, 1984.
- [19] A. Laurain, M. Hintermüller, M. Freiburger, and H. Scharfetter. Topological sensitivity analysis in fluorescence optical tomography. *Inverse Problems*, 29(2):025003,30, 2013.

- [20] A. A. Novotny and J. Sokołowski. *Topological derivatives in shape optimization*. Interaction of Mechanics and Mathematics. Springer, 2013.
- [21] F. Santosa. A level-set approach for inverse problems involving obstacles. *ESAIM Contrôle Optim. Calc. Var.*, 1:17–33, 1995/96.
- [22] Donald Sarason. *Complex function theory*. American Mathematical Society, Providence, RI, second edition, 2007.

(A. Canelas) INSTITUTO DE ESTRUCTURAS Y TRANSPORTE, FACULTAD DE INGENIERÍA, UNIVERSIDAD DE LA REPÚBLICA, AV. JULIO HERRERA Y REISSIG 565, C.P. 11.300, MONTEVIDEO, URUGUAY
E-mail address: `acanelas@fing.edu.uy`

(A. Laurain) INSTITUT FÜR MATHEMATIK, TECHNICAL UNIVERSITY BERLIN, STRASSE DES 17. JUNI 136, 10623 BERLIN, GERMANY
E-mail address: `laurain@math.tu-berlin.de`

(A. A. Novotny) LABORATÓRIO NACIONAL DE COMPUTAÇÃO CIENTÍFICA LNCC/MCT, COORDENAÇÃO DE MATEMÁTICA APLICADA E COMPUTACIONAL, AV. GETÚLIO VARGAS 333, 25651-075 PETRÓPOLIS - RJ, BRASIL
E-mail address: `novotny@lncc.br`